



Single and simultaneous multiple intracerebral hemorrhages: a radiological review

Dimitri Renard¹ · Giovanni Castelnovo¹ · Ioana Ion¹ · Jean Sebastien Guillamo¹ · Eric Thouvenot^{1,2}

Received: 9 May 2019 / Accepted: 14 May 2020 / Published online: 24 May 2020
© Belgian Neurological Society 2020

Abstract

Simultaneous multiple intracerebral hemorrhage (SMICH) is defined as ICH in two or more discrete noncontiguous acute intraparenchymal locations on initial CT. About 5% of ICH patients present with SMICH. ICH/SMICH etiology is classically divided into disorders of primary or secondary origin. About half of primary SMICH cases are caused by cerebral amyloid angiopathy or hypertensive arteriopathy. In this review, we will discuss the radiological features associated with the different causes of primary and secondary ICH and SMICH. Due to its rarity and the associated high morbidity and mortality, we will focus in particular on SMICH.

Keywords Simultaneous · Multiple · Intracerebral hemorrhage

Introduction

About 5% of intracerebral hemorrhage (ICH) patients present with simultaneous multiple ICH (SMICH) [1–6]. SMICH is defined as ICH in two or more discrete noncontiguous acute intraparenchymal locations on initial CT. The etiology of SMICH is classically divided into disorders of primary or secondary origin [1–6]. Sometimes, SMICH is used strictly to refer to primary SMICH. Secondary SMICH is more frequent than primary SMICH. ICH/SMICH can be etiologically classified using the Structural lesion, Medication, Amyloid angiopathy, Systemic/other disease, Hypertension, Undetermined (SMASH-U) classification [7, 8]. In the vast majority of primary SMICH cases, SMICH tends to involve two locations including at least one supratentorial brain area. On initial CT, the exact stage (and thus the true simultaneous character) of the different ICH is sometimes difficult to establish (i.e., the different ICH may be of similar acute stage or of mixed acute/early subacute stage). SMICH is associated with low baseline Glasgow Coma Scale on

admission, female sex, lobar ICH location, cerebral microbleeds (CMB), and renal dysfunction [1, 2]. In the biggest SMICH case series half of primary cases were caused by cerebral amyloid angiopathy (CAA) and hypertensive arteriopathy (HA) with CAA being most common [1]. In contrast, HA predominates over CAA as an etiology of single ICH [1]. Conflicting data on SMICH clinical outcome have been reported. The highest mortality seems to be associated with deep SMICH [3].

SMICH is a rare diagnostic entity that has many different etiologies and is associated with a high level of mortality and morbidity. Consequently, clinicians may feel uneasy when assessing and managing a patient with SMICH. In this review, we will discuss the radiological characteristics of the different underlying disorders causing ICH and SMICH. In clinical practice, the classification as primary and secondary causes of ICH/SMICH is not always straightforward. The first part of this review describes the SMASH-U classification; the second part discusses disorders not specifically determined (or classified as undetermined) by the SMASH-U classification. Table 1 gives an overview of the radiological features frequently associated with each of the different ICH/SMICH etiologies.

✉ Dimitri Renard
dimitrirenard@hotmail.com

¹ Department of Neurology, CHU Nîmes, Hôpital Caremeau, University of Montpellier, 4, Rue Du Pr Debré, 30029 Nîmes Cedex 4, France

² Institut de Génétique Fonctionnelle, UMR 5203, INSERM 1191, Université Montpellier, Montpellier, France

Table 1 Radiological features orientating towards different underlying SMICH etiologies. For each etiology, other frequently associated radiological features are shown

Radiological features	Underlying etiologies	Frequently associated radiological features
Location ICH: -Supratentorial lobar or superficial cerebellar	CAA	Lobar CMB, CSS, posterior leukoencephalopathy, centrum semiovale enlarged perivascular spaces, chronic ICH
	Trauma	Subarachnoid, subdural, extradural, or intraventricular hemorrhage, skull fracture, CMB, DAI, arterial dissection
	Coagulation disorder	Fluid-blood level inside acute ICH, CMB
	Drug abuse	Infarction, aneurysm, arterial stenoses (due to vasculitis or vasospasm), IE-related radiological features
	CVST	Thrombosis of venous structures, finger-like extensions of ICH, mixed vasogenic/cytotoxic edema
Location ICH: -Supratentorial deep, brainstem, or deep cerebellar	CCM	Calcifications, mixed chronic and acute hemorrhage
	HA	Signs of HA-related SVD (BG and brainstem lacunes, internal and external capsules WMH, and BG enlarged perivascular spaces), intraventricular hemorrhage extension
Location ICH: -Bilateral cerebellar	Drug abuse	Infarction, aneurysm, arterial stenoses (due to vasculitis or vasospasm), IE-related radiological features
	RCH	Signs of intracranial hypotension (enhancement of meningeal structures, dilatation of venous structures, extradural hemorrhage, brain sagging, extradural CSF collection)
Finger-like extensions of acute ICH	CAA	Lobar CMB, CSS, posterior leukoencephalopathy, centrum semiovale enlarged perivascular spaces, chronic ICH, SAHE in acute ICH
SAHE	CAA	Lobar CMB, CSS, posterior leukoencephalopathy, centrum semiovale enlarged perivascular spaces, chronic ICH, finger-like extensions in acute ICH
Fluid-blood level	Coagulation disorder	Lobar ICH, CMB related to coagulation disorder
	Anticoagulation therapy	Features related to underlying pathology (e.g., CAA, HA)
	CAA	Lobar CMB, CSS, posterior leukoencephalopathy, centrum semiovale enlarged perivascular spaces, chronic ICH, SAHE and finger-like extension in acute ICH
Calcification of hemorrhagic lesion Contrast enhancement	CCM	Mixed chronic and acute hemorrhage
	Tumor	Other (non-hemorrhagic) contrast-enhancing lesions
	Vasculitis	Multiple arterial stenoses, infarction, CMB, SAH, pseudotumoral lesions, new brain lesions on follow-up imaging
	HT of ischemic infarction	Other areas of infarction, abnormalities associated with the underlying cause of infarction (e.g., vasculitis, IE, moyamoya, intracardiac myxoma)
Signal changes in venous structures	CVST	Thrombosis of venous structures, finger-like extensions of ICH, mixed vasogenic/cytotoxic edema
Aneurysm	Aneurysm rupture-related ICH	ICH in or near basal ganglia, SAH
	IE	Infarction, ICH, CMB (often multiple, and located preferentially in cortical areas), brain abscess, meningitis, hemorrhagic transformation ischemic lesions after IVT
Multiple intracerebral arterial stenoses	Vasculitis	Infarction, CMB, SAH, parenchymal or meningeal enhancement, pseudotumoral lesions, new brain lesions on follow-up imaging
	PRES	Posterior predominant vasogenic edema, vasospasm, CMB, SAH
	MMD	Extensive network of collateral vessels at the base of the brain, infarction, CMB
Simultaneous remote or subsequent infarction	HT of ischemic infarction	Cortical enhancement in the subacute phase, abnormalities associated with the underlying cause of infarction (e.g., vasculitis, IE, moyamoya, intracardiac myxoma)

Table 1 (continued)

Radiological features	Underlying etiologies	Frequently associated radiological features
Vasogenic edema (other than surrounding the ICH)	IE	Mycotic aneurysms, ICH, CMB (often multiple, and located preferentially in cortical areas), brain abscess, meningitis, and hemorrhagic transformation ischemic lesions after IVT
	Vasculitis	Multiple arterial stenosis, CMB, SAH, parenchymal or meningeal enhancement, pseudotumoral lesions, new brain lesions on follow-up imaging
	CVST	Thrombosis of venous structures, finger-like extensions of ICH, mixed vasogenic/cytotoxic edema
	PRES	Posterior predominant vasogenic edema, vasospasm, CMB, SAH

ICH intracerebral hemorrhage, *SAHE* subarachnoid hemorrhage, *CAA* cerebral amyloid angiopathy, *CVST* cerebral venous sinus thrombosis, *CCM* cerebral cavernomatous malformation, *HA* hypertensive arteriopathy, *RCH* remote cerebral/cerebellar hemorrhage, *HT* hemorrhagic transformation, *PRES* posterior reversible encephalopathy syndrome, *MMD* moyamoya disease, *IE* infective endocarditis, *CMB* cerebral microbleeds, *CSS* cortical superficial siderosis, *DAI* diffuse axonal injury, *SVD* small vessel disease, *BG* basal ganglia, *WMH* white matter hyperintensities, *CSF* cerebrospinal fluid, *SAH* subarachnoid hemorrhage, *IVT* intravenous thrombolysis

Underlying ICH/SMICH etiologies

Structural lesion-related ICH/SMICH

Cerebral venous sinus thrombosis

On non-enhanced CT, the venous thrombus can be visualized with increased density, often associated with parenchymal edema (observed with decreased parenchymal density) and ICH (seen with increased parenchymal density, often with a lobar location) or subarachnoid hemorrhage, while CT venography will show the lack of enhancement at the level of the venous thrombus. On MRI, the venous thrombus itself can be observed on T1-weighted imaging (isointense in the acute and hyperintense in the subacute phase), FLAIR (hyperintensity), T2*/susceptibility-weighted imaging (hypointensity with susceptibility-related blooming effect), DWI (hyperintensity), and native 3D-TOF MRA images (hyperintensity) (Fig. 1). Contrast-enhanced MR venography is probably the most reliable sequence to diagnose cerebral venous sinus thrombosis (CVST). On MRI, CVST-related vasogenic edema shows high ADC values, while hemorrhage and cytotoxic edema are typically associated with low or mixed ADC values (Fig. 2). Parenchymal brain lesions (including ICH) related to thrombosis of midline cerebral venous structures (i.e., inferior and superior sagittal sinus, straight sinus, and deep venous system) are often bilaterally and paramedially located.

In case of multiple CVST-related brain lesions, the presence of mixed vasogenic/cytotoxic edema, hemorrhagic infarction, and ICH is often observed, whereas isolated pure SMICH (i.e., in the absence of associated edema and infarction) is rare [9]. Hemorrhagic CVST lesions are frequently seen in the presence of CVST located in the sigmoid

or straight sinus or in case of multiple venous sinus thromboses [9, 10]. Other features associated with CVST-related hemorrhage include advanced age, headache, behavioral disturbances, impaired consciousness, seizures, language deficit, high blood pressure on admission, puerperium, and worse clinical outcome [9].

CVST must be ruled out (especially as the underlying disorder is treatable) in SMICH patients presenting with headache, seizures, infections with parameningeal locations, and signal changes in the cerebral venous structures and associated vasogenic edema and infarction on brain imaging.

Cerebral cavernous malformation

Sporadic cerebral cavernous malformations (CCM) are generally single isolated lesions, whereas familial CCM (due to mutations in the *CCM1*, *CCM2*, or *CCM3* gene) is often associated with multiple lesions. The most frequent clinical manifestations of CCM are seizures and focal neurological deficit due to hemorrhage. The overall bleeding risk of CCM is relatively low. Therefore, CCM-related hemorrhage presents as a single ICH in the vast majority of cases. Some rare cases of CCM-related SMICH have been reported [11]. Inflammatory processes and pressure-related phenomena have been suspected to play a role in CMM-related SMICH. CCM, associated chronic and acute bleeding, and CCM-related calcifications are best detected by T2*- and susceptibility-weighted imaging (often showing a prominent susceptibility “blooming” effect). CT can easily distinguish hemorrhage (hyperdense in the acute phase, and iso- to hypodense in the chronic phase) from calcifications (showing very high densities with corresponding Hounsfield units, stable over time). On MRI, mixed signal on T1- and T2-weighted imaging

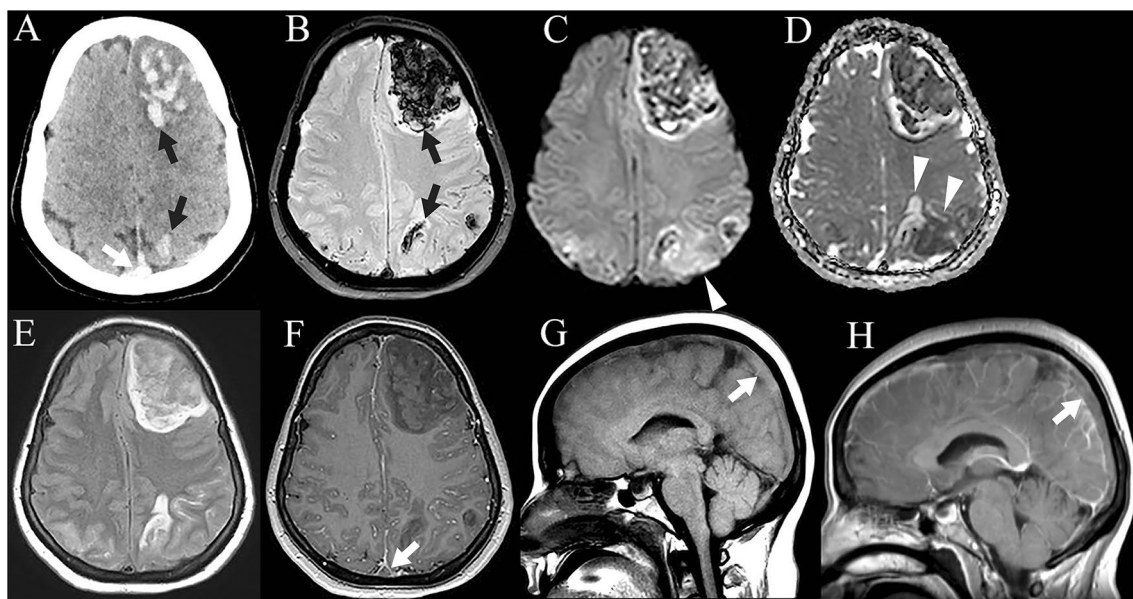
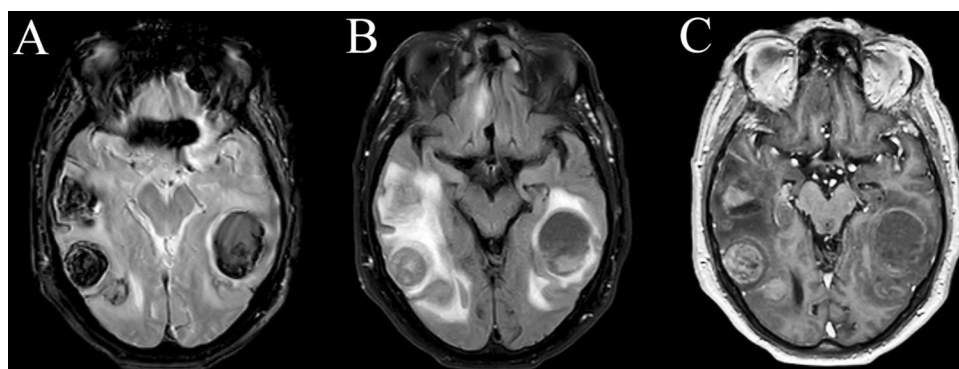


Fig. 1 Brain imaging of a patient with SMICH (black arrows on non-enhanced CT [a] and T2*-weighted MR imaging [b]) related to CVST of the superior sagittal sinus. The CVST is seen as hyperdensity on non-enhanced CT (a, white arrow), iso/hyperintensity on sagittal T1-weighted imaging (g), and with lack of enhancement on gadolinium-enhanced T1-weighted imaging [white arrows on F and H, axial and sagittal gadolinium-enhanced T1-weighted imaging,

respectively]). Associated left parietal edema can be observed on DWI (c), ADC map (d), and FLAIR (e), clearly presenting the mixed cytotoxic (hypointense) and vasogenic (hyperintense) edema on ADC map (d). Associated CVST-related subarachnoid hemorrhage is seen as hypointensity on T2*-weighted imaging (b) and as hyperintensity on FLAIR (e)

Fig. 2 MRI of a patient with multiple large hemorrhagic brain melanoma metastases, with the hemorrhages seen as hypointensities on T2*-weighted imaging (a), associated with surrounding edema seen as hyperintensities on FLAIR (b) and contrast enhancement on gadolinium-enhanced T1-weighted images (c)



with a reticulated so-called “popcorn-like” appearance is suggestive of mixed chronic and acute hemorrhage related to CCM. Gadolinium-injected T1-weighted imaging typically shows no or minimal enhancement.

CCM-related SMICH should be suspected when multiple lesions compatible with CMM are observed on imaging (i.e., lesions with mixed acute and chronic hemorrhage, and calcifications) and family history of CCM evokes the inherited form of CCM.

Rupture of aneurysm

Bleeding due to the rupture of an aneurysm is associated with subarachnoid hemorrhage in the vast majority of cases. Aneurysm rupture-related ICH (often associated with subarachnoid hemorrhage) typically occurs in or near the basal ganglia, related to rupture of a distal lenticulostriate artery aneurysm. Very rare SMICH cases related to simultaneous rupture of multiple aneurysms have been reported [12]. In

patients with multiple aneurysms, arterial pressure- and inflammatory-related processes were suspected to explain simultaneous rupture of these aneurysms. Especially in young patients without history of hypertension, aneurysm-related ICH must be suspected and detailed vessel imaging has to be performed in the presence of a perisylvian location of ICH, subacute ICH expansion or ICH recurrence, and associated subarachnoid hemorrhage.

Tumor

Due to increased tumor vascularization with dilated thin-walled vessels and tumor necrosis, brain tumors may be associated with hemorrhage. The most common primary brain tumors associated with hemorrhage are pituitary adenomas, meningiomas, and high-grade gliomas [13]. The most frequent metastatic hemorrhagic brain tumors include malignant melanoma, thyroid, renal cell, hepatocellular, and lung cancers [13]. Rarely, CNS germinoma, ependymoma, choroid plexus carcinoma, pineocytoma, and metastatic choriocarcinoma and germ cell tumors may present with tumor-related hemorrhage. In patients with brain tumors and associated venous thromboembolism treated with therapeutic anticoagulation, increased risk for ICH is especially observed in patients with primary brain tumors (e.g., glioma) as opposed to metastatic brain tumors [14].

In case of tumor-related SMICH, a high number of hemorrhagic lesions often is observed, related to metastatic tumors in the majority of cases (Fig. 2). Since these hemorrhagic metastases are often small-sized, and therefore, easily missed on CT, T2*- and susceptibility-weighted MRI sequences are the best choice to detect small hemorrhagic lesions [15]. After gadolinium injection, ring-enhancement is often observed in these hemorrhagic tumor lesions on T1-weighted imaging (Fig. 2).

Tumor-related SMICH should be suspected in the presence of a high number of small (and sometimes larger) hemorrhagic lesions showing contrast enhancement. Special attention has to be paid to patients with brain metastases treated with bevacizumab, since this treatment is associated with high ICH risk [16].

In brain tumor patients treated with radiotherapy, hemorrhagic tumor lesions must be distinguished from radiotherapy-related hemorrhagic lesions (i.e., CMB and cavernomatous malformations) typically seen as small lesions appearing months or years after radiotherapy.

Infective endocarditis

Brain involvement frequently observed in infective endocarditis (IE) includes infarction (often multiple, asymptomatic, affecting cortical and border zone arterial territories), mycotic aneurysms (usually multiple, bilateral, distal, and

fusiform), ICH, CMB, often multiple, and located preferentially in cortical areas and less frequently in the subcortical white matter, the basal ganglia, or the posterior fossa), brain abscess, and meningitis [17, 18]. Hemorrhagic brain lesions in IE can be related to hemorrhagic transformation of infarction (especially after thrombolytic therapy), primary ICH, rupture of infectious cerebral mycotic aneurysms, or suppurative necrotizing focal arteritis. T2*- and susceptibility-weighted imaging are the MRI sequences of choice to detect CMB, small distal aneurysms, and ICH. On MRI, brain abscess is characterized by central restricted diffusion on diffusion-weighted imaging, perilesional FLAIR hyperintensity related to edema, and annular enhancement on gadolinium-injected T1-weighted imaging. The presence of more than two CMB has been shown to be a risk factor for subsequent symptomatic ICH in IE.

In SMICH patients, IE must be suspected in the presence of associated infarctions on diffusion-weighted imaging, small T2*-weighted lesions suggestive of CMB, distal aneurysms, and in acute infarction patients treated by intravenous thrombolysis followed by hemorrhagic transformation of different multiterritorial ischemic lesions.

Acute hemorrhagic leukoencephalitis

Acute hemorrhagic leukoencephalitis (AHLE) is a rare hemorrhagic variant of acute demyelinating encephalomyelitis with a fulminant course and poor prognosis [19]. AHLE generally affects children presenting with rapid neurologic deterioration with death from edema and herniation within a few days or weeks. Brain MRI shows multiple lesions associated with gadolinium enhancement, edema, and hemorrhage. Brain lesions are most often located in the supratentorial area but may also occur in the brainstem and the cerebellum. In addition to hemorrhages, acute demyelination can be suggested by restricted diffusion with corresponding low ADC values. Neuropathology reveals the early presence of hemorrhages, vessel fibrinoid necrosis, perivascular fibrin exudation, edema and neutrophilic inflammation, followed by perivascular demyelination, microglial foci and myelin-laden macrophages.

Hemorrhagic transformation of ischemic infarction

Independent risk factors for hemorrhagic transformation (HT) of ischemic infarction include large infarct size, stroke severity, large-artery occlusion (especially the hyperdense middle cerebral artery sign), cardioembolism, and thrombolytic therapy [20, 21]. Other parameters may also play a role in HT including older age, pre-treatment with antiplatelet or anticoagulant agents, anterior circulation infarction, poor baseline collaterals, fever, hyperglycemia, low serum cholesterol, elevated blood pressure in the acute setting,

renal insufficiency, low platelet count, elevated globulin level, high white blood cell count, and albuminuria. HT is clinically classified as symptomatic or asymptomatic, and radiologically as hemorrhagic infarction type 1 (petechial hemorrhages at the infarct margins), hemorrhagic infarction type 2 (petechial hemorrhages throughout the infarct without mass effect), parenchymal hematoma type 1 (involving < 30% of the infarcted area with minor mass effect attributable to the hematoma), and parenchymal hematoma type 2 (involving > 30% of the infarct zone with substantial mass effect attributable to the hematoma, and associated with poor clinical outcome) according to the European Cooperative Acute Stroke Study (ECASS) II.

HT-related SMICH may be observed in patients with multifocal or multiterritorial infarction (generally of embolic origin) and in the presence of associated risk factors for HT. HT-related-SMICH (corresponding to parenchymal hematoma HT type) typically occurs in brain areas corresponding to arterial territories and in infarction areas observed on initial brain imaging (highly visible on MRI in the hyperacute phase) although new subsequent infarctions with HT can be encountered in high risk patients (e.g., intraluminal artery thrombus, high degree arterial stenosis, IE, intracardiac thrombus or myxoma). In patients with parenchymal hematoma type 2 on control MRI without available acute phase MRI showing initial infarction, diffusion-weighted imaging is often of limited use, since hemorrhage-related mixed signal masks the initial homogeneous increased DWI signal and decreased ADC values. In these cases, the presence of cortical enhancement on gadolinium-injected T1-weighted imaging may be helpful to identify initial underlying infarction. In HT-related SMICH patients, underlying etiologies associated with frequent hemorrhagic stroke should be suspected (e.g., vasculitis, IE, intracardiac myxoma, or moyamoya disease).

Vasculitis

Radiological features observed in vasculitis include arterial abnormalities (irregularities, segmental stenoses, and occlusions with an atypical pattern for atherosclerosis disease), infarctions, hemorrhagic lesions (CMB, subarachnoid hemorrhage, and ICH), T2/FLAIR hyperintensities, pseudotumoral lesions, and gadolinium enhancement of parenchymal lesions or leptomeningeal structures. Primary angiitis of the CNS typically affects small- and medium-sized arteries. These arterial abnormalities can be best seen on digital subtraction angiography (although sometimes false negative), but sometimes also on CTA and MRA. In vasculitis, a mix of recent infarctions, subacute/chronic infarctions, and hemorrhages are frequently observed.

In SMICH patients, underlying vasculitis should be suspected in the presence of associated infarctions, CMB,

gadolinium enhancement, and/or multifocal arterial abnormalities, and in case of new brain lesions on follow-up brain imaging [22].

Moyamoya disease

Moyamoya disease (MMD) is a rare idiopathic occlusive cerebrovascular disorder characterized by progressive stenosis or occlusion of the distal internal carotid artery or its proximal branches and an extensive network of collateral vessels at the base of the brain. MMD is associated with infarction, ICH, and CMB. ICH and CMB are thought to be related to abnormal, expanded and distorted lenticulostriate and thalamoperforate arteries manifesting internal elastic layer fracture and medial fibrosis. Very rare cases of MMD-related SMICH have been reported [23]. CMB are a predictor of future ICH in MMD. Hemorrhagic MMD complications are more frequent in patients of Asian descent (showing CMB predominantly in the deep grey nuclei and the periventricular region) than in European MMD patients (with CMB predominant in the cortex and the grey-white matter junction).

MMD-related SMICH must be suspected in case of severe stenosis of the distal internal carotid arteries, often in the presence of associated infarction and/or CMB.

Medication-related ICH/SMICH

Anticoagulation therapy

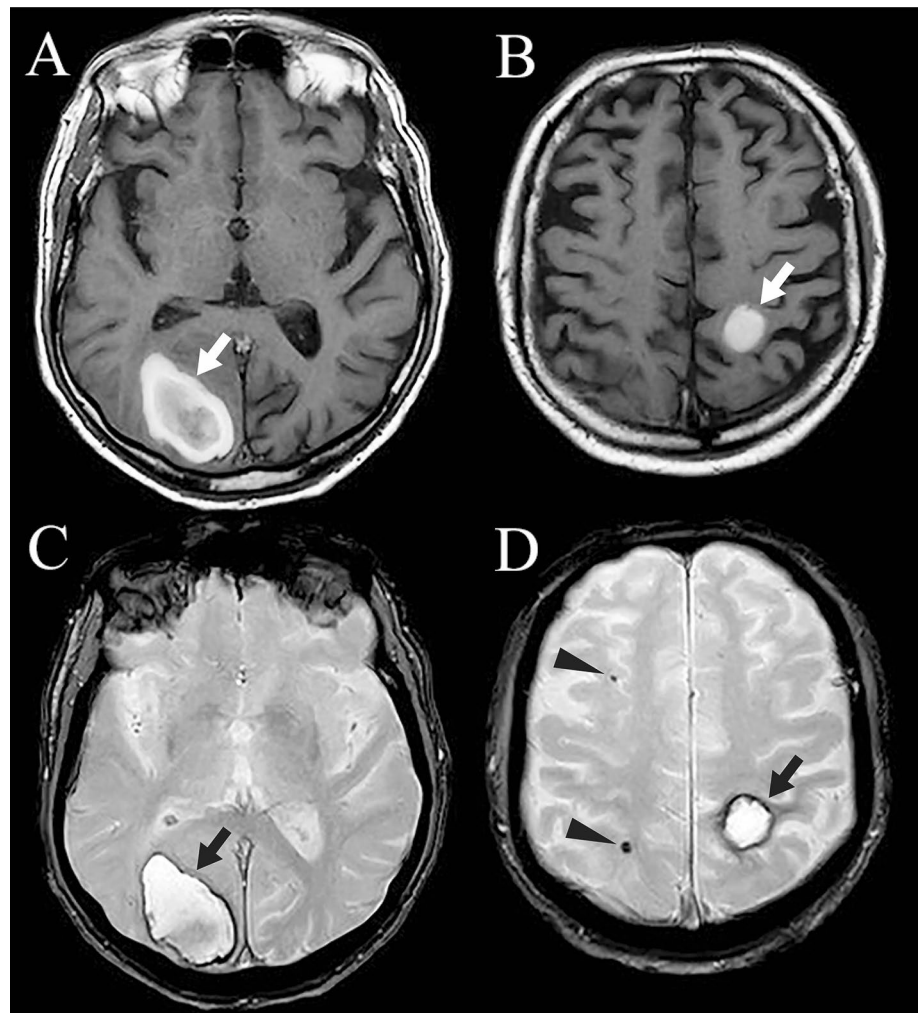
In patients receiving anticoagulation therapy (e.g., warfarin, new oral anticoagulants, full-dose heparin), both deep and lobar ICH can be encountered, probably due to unmasking of an underlying disease (e.g., CAA or HA, probably explaining the deep grey matter of lobar distribution of these anticoagulation-related ICH). Therefore, in SMICH patients treated with anticoagulation therapy, radiological features related to an underlying arterial disorder must be analyzed (Fig. 3).

Although not completely specific (also reported in CAA and CVST), a fluid-blood level inside the ICH can often be observed on initial brain imaging in patients with ICH related to a coagulation disorder or anticoagulation therapy [24].

Remote parenchymal hemorrhages after intravenous thrombolysis

Remote parenchymal hemorrhages (RPH), including CMB and ICH, are defined as single or multiple hemorrhages appearing in brain regions without visible ischemic damage detected by brain imaging, remote from the area causing initial stroke symptoms. RPH is associated with

Fig. 3 MRI performed in the subacute phase of a patient treated with warfarine for atrial fibrillation presenting with SMICH. T1-weighted imaging (a, b) shows the subacute ICH (arrows) as hyperintensities in the right occipital and left parietal lobe and as lesions with peripheral hypointensity on T2*-weighted imaging (c, d). The presence of two chronic isolated cortical microbleeds on T2*-weighted imaging are in favor of underlying CAA etiology



poor outcome. Suspected underlying mechanisms include undiagnosed coagulopathies, multiple acute embolic areas of ischemia, and generalized cerebral vasculopathy (e.g., CAA) [25, 26]. In the largest observational multicenter study on RPH, lobar CMB (indicative of CAA-related vasculopathy) and recent silent ischemia were independent risk factors for RPH [26]. In patients with remote ICH following intravenous thrombolysis, associated remote CMB are frequently observed. RPH location is more commonly lobar than deep or infratentorial, further supporting underlying CAA-related pathophysiology. Another large study showed that lobar RPH was associated with imaging markers of amyloid deposition, whereas high blood pressure within the first 24 h after intravenous thrombolysis was associated with deep RPH, suggesting that deep and lobar RPH after intravenous thrombolysis may have different mechanisms [27].

RPH-related SMICH must be suspected in stroke patients with chronic pre-existing lobar ICH or CMB, presenting with subsequent remote lobar ICH after intravenous thrombolysis.

Cerebral amyloid angiopathy

CAA is caused by the accumulation of β -amyloid protein in the walls of cortical and leptomeningeal arteries. On MRI, CAA is associated with the presence of lobar supratentorial (and sometimes superficial cerebellar) ICH, lobar CMB (predominantly observed in the cortex, and sparing deep grey matter and brain stem, and to a lesser degree, the superficial cerebellum), acute convexity subarachnoid hemorrhage, cortical superficial siderosis, subcortical and cortical (often silent) infarctions, centrum semiovale enlarged perivascular spaces, cortical and subcortical atrophy, and white matter hyperintensities predominant in the posterior regions and with a “multiple subcortical spots” pattern (Fig. 4). The lobar ICH and CMB in CAA are characterized by a predilection for the posterior brain regions. In patients with advanced CAA, there is an inverted association between cortical superficial siderosis severity and CMB numbers. Diagnostic CAA criteria are (together with age > 55 years) largely based on the presence of lobar ICH, cortical superficial siderosis, and CMB [28]. CAA-related hemorrhagic

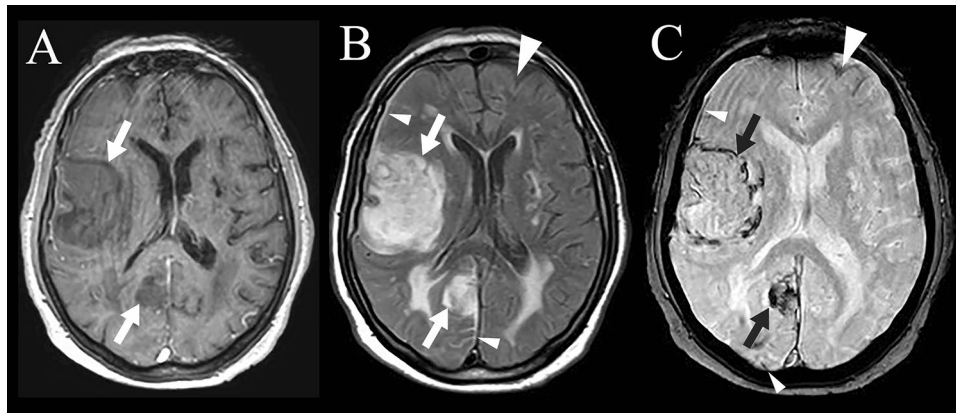


Fig. 4 Gadolinium-enhanced T1-weighted (a), FLAIR (b), and T2*-weighted imaging (c) showing SMICH (arrows). The MRI performed in the acute phase shows SMICH (arrows) as isointensity on T1-weighted imaging (a), hyperintensity on FLAIR (b), and with peripheral hypointensity on T2*-weighted images (c). Hence the acute subarachnoid hemorrhage diffusion of SMICH seen as hyper-

intensity on FLAIR (b, small arrowheads) and hypointensity on T2*-weighted imaging (c, small arrowheads), the presence of chronic cortical superficial siderosis (seen as hypointensity on T2*-weighted imaging, without signal changes on FLAIR, large arrowheads), and posterior predominant leukoencephalopathy, all evoking CAA as underlying SMICH cause in this patient

features are best seen on T2*- and susceptibility-weighted imaging. In patients with acute ICH, the presence of finger-like projections and subarachnoid hemorrhage extension on CT (together with the presence of ApoE4 genotype) are associated with CAA pathology. The risk of ICH in CAA is associated with the presence of chronic ICH, high CMB number, cortical superficial siderosis (especially when multifocal), extensive (periventricular Fazekas score of 2–3 or total Fazekas score of 5–6) white matter hyperintensities, the use of anticoagulation therapy, and potentially also the ApoE2 genotype and associated CAA-related inflammation [26, 29–31]. Risk factors for SMICH in CAA have not been specifically studied.

CAA-related SMICH should be suspected in older patients in case of multiple supratentorial lobar or mixed supratentorial lobar/superficial cerebellar ICH, especially when associated with other typical radiological CAA features.

Systemic disease-related ICH/SMICH

Systemic disease-related ICH/SMICH includes chronic kidney disease, thrombocytopenia, liver disease, and nondrug-induced coagulopathy. In patients with hematologic disorders, the presence of ICH (often associated with CMB) is frequently reported in acute myeloid leukemia and aplastic anemia, and associated with a high mortality rate [32–34]. The most frequent ICH location is the cortex, with the parietal lobe as the most frequently involved brain area. Frequently, a single ICH is observed although coagulopathy-related SMICH cases have been reported. In acute myeloid leukemia, risk factors for ICH include high peripheral white blood count, low peripheral platelet count, low albumin and

fibrous protein levels, and prolongation of prothrombin time. In acute leukemia patients, ICH can also be related to CVST, with a possible role of asparaginase treatment [35]. Ecchymosis, upper gastrointestinal hemorrhage, hematuria, and low platelet count are associated with ICH in aplastic anemia patients. Disorders such as disseminated intravascular coagulation and idiopathic thrombocytopenic purpura are more frequently associated with CMB than with ICH.

ICH and SMICH can be encountered in other systemic coagulopathies, like in patients with low platelet count and hepatic cirrhosis (especially when alcohol-related, due to associated thrombocytopenia and coagulation abnormalities).

Hypertensive arteriopathy

Hypertension causes arteriolosclerosis in both cortical and subcortical small arteries and arterioles. On MRI, hypertensive arteriopathy (HA) is associated with the presence of ICH and CMB typically located in the deep grey matter, brain stem, and deep cerebellum, enlarged perivascular spaces predominant in the basal ganglia, infarctions (especially lacunes, with a predilection for the basal ganglia and the brain stem), white matter hyperintensities (typically involving the internal and external capsules and the brain stem), and dolichoectasia of cerebral arteries. HA-related ICH are often associated with intraventricular hemorrhage extension.

In SMICH patients with a history of hypertension, underlying HA must be suspected when ICH are located in the basal ganglia, the thalamus, the brain stem, or the deep cerebellum, especially in the presence of other MRI features suggestive of HA-related small vessel disease [1, 3, 36, 37].

In young SMICH patients with severe hypertension, secondary causes of arterial hypertension (e.g., obstructive sleep apnea, renal parenchymal disease, renal artery stenosis, or primary aldosteronism) should be suspected and ruled out.

Other determined causes of ICH/SMICH

Drug abuse

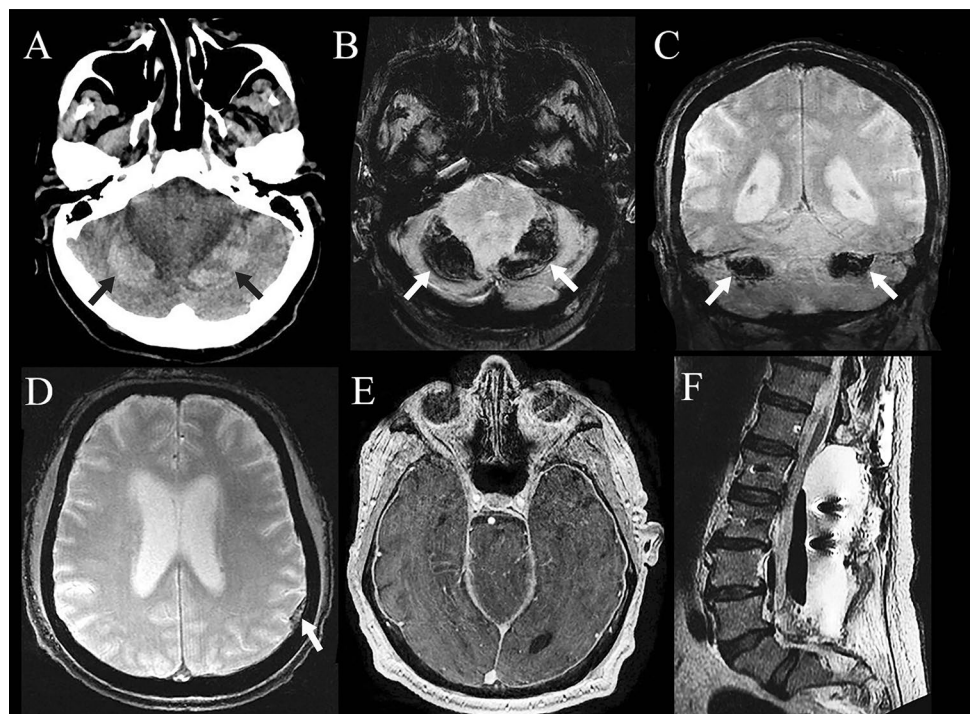
Illicit drug-related hemorrhage (including single, multiple or mixed ICH, subarachnoid, or intraventricular hemorrhage) is associated with the use of amphetamine, cocaine, or ecstasy (all having sympathomimetic effects in common) in the majority of cases, while association with others drugs such as cannabis, pentazocine, phencyclidine, phenylpropanolamine, pyribenzamine, methylphenidate, and phosphodiesterase inhibitors has also been reported [38, 39]. Mechanisms possibly playing a role in these drug-related hemorrhages include hypertension surges, underlying aneurysm, vasculitis, hemorrhagic transformation of ischemic infarcts, and changes in cerebrovascular autoregulation. Cocaine-related ICH typically shows a subcortical location, while amphetamine-related ICH can be subcortical or lobar. Illicit drug use has also been associated with reversible cerebral vasoconstriction syndrome (to be suspected in case of recurrent thunderclap headache), sometimes complicated with infarction, hemorrhagic infarction, ICH, or subarachnoid hemorrhage. Infarction or hemorrhagic infarction can be also observed in case of drug-related cardioembolism (due to IE, foreign substances in intravenous drug users, or

cardiac arrhythmia). In illicit drug-related SMICH, other brain abnormalities related to drug abuse should be assessed, including infarction, aneurysm, arterial stenosis (due to vasculitis or vasospasm), and IE-related brain complications.

Remote cerebral/cerebellar hemorrhage

Remote cerebral and cerebellar hemorrhage (RCH) is defined by bleeding as a complication of surgery performed at a location distant from the site of bleeding. RCH can be seen after both spinal and cranial surgery. Risk factors for RCH after supratentorial craniotomies include surgery for intracranial aneurysms, tumor debulking, and lobectomies, coagulation disorders, perioperative CSF leakage, hypertension, and seizures [40]. After spinal procedures, RCH is associated with decompressive procedures for spinal canal stenosis (particularly when associated with instrumental fusion), spinal tumor debulking, and disc herniation removal, coagulation disorders, hypertension, and placement of postoperative subfascial drainages [41, 42]. The most frequent RCH location is the cerebellum (most often bilateral, showing the so-called “zebra sign” on CT with hyperdense curvilinear hemorrhage between hypodense cerebellar folia), followed by supratentorial ICH location (Fig. 5). Although sometimes asymptomatic, RCH is associated with impairment of consciousness in the majority of cases. CSF leakage and intracranial hypotension are thought to play a major causative role in RCH through an increase in the transmural venous pressure, resulting in blood vessel rupture, and downward cerebellar sag causing stretching and

Fig. 5 MRI performed after recent decompressive spinal surgery (associated with instrumental fusion) for lumbar canal stenosis in a patient presenting with impairment of consciousness and orthostatic headache, showing bilateral cerebellar ICH on axial CT (a) and on axial and coronal T2*-weighted imaging (b, c). Intracranial hypotension MRI features including extradural hemorrhage (d, T2*-weighted image) and diffuse meningeal enhancement after gadolinium injection (E, gadolinium-enhanced T1-weighted imaging) can be seen, caused by a large surgery-related extradural lumbar CSF collection (F, sagittal T2-weighted imaging)



occlusion of the bridging cerebellar veins with subsequent hemorrhagic venous infarction. MRI features of intracranial hypotension include enhancement of meningeal structures after gadolinium injection, dilation of the cerebral venous structures, extradural CSF collection, extradural hemorrhage, and sometimes brain sagging (Fig. 5).

RCH-related SMICH should be suspected when occurring after recent cranial or spinal surgery, in the presence of clinical (e.g., orthostatic headache) and radiological signs of intracranial hypotension.

Posterior reversible encephalopathy syndrome

Posterior reversible encephalopathy syndrome (PRES) refers to a disorder of reversible subcortical vasogenic edema predominant in the posterior brain regions, frequently associated with brain stem, basal ganglia, and/or cerebellar involvement. Patients typically present with neurological symptoms including seizures, encephalopathy, headache, and visual disturbances. PRES is often associated with high blood pressure, (pre-)eclampsia, cytotoxic drugs, renal failure, and autoimmune disorders. On MRI, in addition to the presence of typical vasogenic edema, associated restricted diffusion (representing cytotoxic edema) and hemorrhagic complications (including ICH, subarachnoid hemorrhage, and CMB) can be observed in severe PRES and seem to be associated with worse functional outcome [43, 44]. ICH has been observed in up to 20% of PRES cases, with multiple hemorrhagic foci in more than half of cases. These hemorrhagic complications are particularly frequent in PRES patients with associated high blood pressure, ongoing therapeutic anticoagulation, and intrinsic coagulopathy. When systematically searched for by susceptibility-weighted imaging sequences, CMB (generally present in low numbers) are observed in 58% of PRES patients, particularly PRES patients with other extensive PRES-related MRI abnormalities.

In PRES-related SMICH patients, focal neurological deficit due to ICH is usually preceded by headache, encephalopathy, seizures, or visual disturbances, and associated with the presence of vasogenic edema predominant in the posterior brain regions on MRI.

Trauma

Cranial lesions frequently observed after blunt head trauma include contusion, skull fracture, ICH, CMB, subarachnoid, subdural, extradural, or intraventricular hemorrhage, arterial dissection, and diffuse axonal injury in case of severe head trauma. SMICH caused by head trauma is generally associated with other types of trauma-related cranial lesions. Trauma-related ICH is more often lobar than deep, with preferential involvement of the frontal (especially frontobasal)

and temporal (especially the anterior part) lobes [45]. Diffuse axonal injury typically involves the corpus callosum, the midbrain, and the lobar white matter (most often at the grey-white matter junction), and is best seen on diffusion-weighted imaging and FLAIR sequences as hyperintense signal frequently associated with CMB on T2*-weighted imaging.

Generally, the diagnosis of trauma-related SMICH is straightforward because of the history of recent head trauma and the presence of other trauma-related radiological cranial abnormalities. However, sometimes primary ICH can lead to head trauma (e.g., due to a fall or a car accident) and the simultaneous presence of both primary ICH and trauma-related brain lesions on brain imaging make interpretation of radiological abnormalities more difficult.

Conclusion

A multitude of underlying disorders give rise to ICH/SMICH. Diagnosis largely relies on radiological features. Complete brain imaging (including unenhanced and contrast-enhanced CT, and MRI including FLAIR, diffusion-, T2-, T2*-, unenhanced and gadolinium-enhanced T1-weighted imaging, and MRA) is needed to detect different radiological abnormalities frequently associated with each of the different underlying disorders causing SMICH.

Acknowledgements We would like to thank Dr. Sarah Kabani (Service de Biostatistique, Epidémiologie Clinique, Santé Publique et Innovation en Méthodologie (BESPIM), CHU de Nîmes, 4 Rue du Professeur Debré, 30029 Nîmes Cedex 09) for proofreading our manuscript.

Compliance with ethical standards

Conflict of interest We have no conflict of interest to declare.

Ethical statement The subject has given her informed consent to report data given. The manuscript was approved by the institute's committee on human research.

References

1. Wu TY, Yassi N, Shah DG et al (2017) Simultaneous Multiple Intracerebral Hemorrhages (SMICH). *Stroke* 48:581–586
2. Stemer A, Ouyang B, Lee VH et al (2010) Prevalence and risk factors for multiple simultaneous intracerebral hemorrhages. *Cerebrovasc Dis* 30:302–307
3. Laiwattana D, Sangsawang B, Sangsawang N (2014) Primary Multiple Simultaneous Intracerebral Hemorrhages between 1950 and 2013: analysis of Data on Age, Sex and Outcome. *Cerebrovasc Dis Extra* 4:102–114
4. Seo JS, Nam TK, Kwon JT et al (2014) Multiple spontaneous simultaneous intracerebral hemorrhages. *J Cerebrovasc Endovasc Neurosurg* 16:104–111

5. Chen Y, Hénon H, Bombois S et al (2016) Multiple simultaneous spontaneous intracerebral hemorrhages: a rare entity. *Cerebrovasc Dis* 41:74–79
6. Yamaguchi Y, Takeda R, Kikkawa Y et al (2017) Multiple simultaneous intracerebral hemorrhages: clinical presentations and risk factors. *J Neurol Sci* 383:35–38
7. Meretoja A, Strbian D, Putaala J et al (2012) SMASH-U: a proposal for etiologic classification of intracerebral hemorrhage. *Stroke* 43:2592–2597
8. Yeh SJ, Tang SC, Tsai LK et al (2014) Pathogenetical subtypes of recurrent intracerebral hemorrhage: designations by SMASH-U classification system. *Stroke* 45:2636–2642
9. Kumral E, Polat F, Uzunköprü C et al (2012) The clinical spectrum of intracerebral hematoma, hemorrhagic infarct, non-hemorrhagic infarct, and non-lesional venous stroke in patients with cerebral sinus-venous thrombosis. *Eur J Neurol* 19:537–543
10. Zhou G, Li M, Zhu Y et al (2016) Cerebral venous sinus thrombosis involving the straight sinus may result in infarction and/or hemorrhage. *Eur Neurol* 75:257–262
11. Louis N, Marsh R (2016) Simultaneous and sequential hemorrhage of multiple cerebral cavernous malformations: a case report. *J Med Case Rep* 10:36
12. Havakeshian S, Bozinov O, Burkhardt JK (2013) Simultaneous rupture of two middle cerebral artery aneurysms presented with two aneurysm-associated intracerebral hemorrhages. *J Neurol Surg A Cent Eur Neurosurg* 74(Suppl 1):e233–e236
13. Rogers LR (2008) *Handbook of neuro-oncology neuroimaging*. Academic Press, New York, pp 72–73
14. Zwicker JJ, Karp Leaf R, Carrier M (2016) A meta-analysis of intracranial hemorrhage in patients with brain tumors receiving therapeutic anticoagulation. *J Thromb Haemost* 14:1736–1740
15. Franceschi AM, Moschos SJ, Anders CK et al (2016) Use of susceptibility-weighted imaging (SWI) in the detection of brain hemorrhagic metastases from breast cancer and melanoma. *J Comput Assist Tomogr* 40:803–805
16. Yang L, Chen CJ, Guo XL et al (2018) Bevacizumab and risk of intracranial hemorrhage in patients with brain metastases: a meta-analysis. *J Neurooncol* 137:49–56
17. Silver B, Behrouz R, Silliman S (2016) Bacterial endocarditis and cerebrovascular disease. *Curr Neurol Neurosci Rep* 16:104
18. Asaithambi G, Adil MM, Qureshi AI (2013) Thrombolysis for ischemic stroke associated with infective endocarditis: results from the nationwide inpatient sample. *Stroke* 44:2917–2919
19. Mader I, Wolff M, Niemann G et al (2004) Acute haemorrhagic encephalomyelitis (AHM): MRI findings. *Neuropediatrics* 35:143–146
20. Zhang J, Yang Y, Sun H et al (2014) Hemorrhagic transformation after cerebral infarction: current concepts and challenges. *Ann Transl Med* 2:81
21. Kalinin MN, Khasanova DR, Ibatullin MM (2017) The hemorrhagic transformation index score: a prediction tool in middle cerebral artery ischemic stroke. *BMC Neurol* 17:177
22. Kato E, Tahara K, Hayashi H et al (2018) Granulomatosis with polyangiitis complicated by hypertrophic pachymeningitis presenting with simultaneous multiple intracerebral hemorrhages. *Intern Med* 57:1167–1172
23. Yu J, Yuan Y, Li W et al (2016) Moyamoya disease manifested as multiple simultaneous intracerebral hemorrhages: a case report and literature review. *Exp Ther Med* 12:1440–1444
24. Pflieger MJ, Hardee EP, Contant CF Jr et al (1994) Sensitivity and specificity of fluid-blood levels for coagulopathy in acute intracerebral hematomas. *AJNR Am J Neuroradiol* 15:217–223
25. Prats-Sánchez L, Camps-Renom P, Sotoca-Fernández J, Catalan Stroke Code and Reperfusion Consortium (Cat-SCR) et al (2016) Remote intracerebral hemorrhage after intravenous thrombolysis: results from a multicenter study. *Stroke* 47:2003–2009
26. Braemswig TB, Villringer K, Turc G et al (2019) Predictors of new remote cerebral microbleeds after IV thrombolysis for ischemic stroke. *Neurology* 92:e630–e638
27. Prats-Sánchez L, Martínez-Domeño A, Camps-Renom P et al (2017) Risk factors are different for deep and lobar remote hemorrhages after intravenous thrombolysis. *PLoS One* 12:e0178284
28. Linn J, Halpin A, Demaerel P et al (2010) Prevalence of superficial siderosis in patients with cerebral amyloid angiopathy. *Neurology* 74:1346–1350
29. Charidimou A, Boulouis G, Xiong L et al (2017) Cortical superficial siderosis and first-ever cerebral hemorrhage in cerebral amyloid angiopathy. *Neurology* 88:1607–1614
30. Charidimou A, Imaizumi T, Moulin S et al (2017) Brain hemorrhage recurrence, small vessel disease type, and cerebral microbleeds: a meta-analysis. *Neurology* 89:820–829
31. Charidimou A, Boulouis G, Roongpiboonsopit D et al (2017) Cortical superficial siderosis multifocality in cerebral amyloid angiopathy: a prospective study. *Neurology* 89:2128–2135
32. Quinones-Hinojosa A, Gulati M, Singh V et al (2003) Spontaneous intracerebral hemorrhage due to coagulation disorders. *Neurosurg Focus* 15:E3
33. Zhang Q, Li X, Wei Z et al (2017) Risk factors and clinical characteristics of non-promyelocytic acute myeloid leukemia of intracerebral hemorrhage: a single center study in China. *J Clin Neurosci* 44:203–206
34. Owattanapanich W, Auewarakul CU (2016) Intracranial hemorrhage in patients with hematologic disorders: prevalence and predictive factors. *J Med Assoc Thai* 99:15–24
35. Roininen S, Laine O, Kauppila M et al (2017) A minor role of asparaginase in predisposing to cerebral venous thromboses in adult acute lymphoblastic leukemia patients. *Cancer Med* 6:1275–1285
36. Kumar NS, Neeraja V, Raju CG et al (2015) Multiple spontaneous hypertensive intracerebral hemorrhages. *J Stroke Cerebrovasc Dis* 24:e25–e27
37. Takeuchi S, Takasato Y, Masaoka H et al (2011) Simultaneous multiple hypertensive intracranial hemorrhages. *J Clin Neurosci* 18:1215–1218
38. Pozzi M, Roccatagliata D, Sterzi R (2008) Drug abuse and intracranial hemorrhage. *Neurol Sci* 29(Suppl 2):S269–S270
39. Fonseca AC, Ferro JM (2016) Drug abuse and stroke. *Curr Neurol Neurosci Rep*. 13:325
40. Sturiale CL, Rossetto M, Ermani M et al (2016) Remote cerebellar hemorrhage after supratentorial procedures (part 1): a systematic review. *Neurosurg Rev* 39:565–573
41. Sturiale CL, Rossetto M, Ermani M et al (2016) Remote cerebellar hemorrhage after spinal procedures (part 2): a systematic review. *Neurosurg Rev* 39:369–376
42. You SH, Son KR, Lee NJ et al (2012) Remote cerebral and cerebellar hemorrhage after massive cerebrospinal fluid leakage. *J Korean Neurosurg Soc* 51:240–243
43. Garcha M, Sivakumar K, El-Hunjul M et al (2018) Intracranial hemorrhage in the setting of posterior reversible encephalopathy syndrome: two case reports and a review. *Hosp Pract* 46:103–109
44. Babi MA, Gorman MJ, Cipolla MJ et al (2016) Ondansetron-related hemorrhagic posterior reversible encephalopathy syndrome (PRES) following gastric bypass. *Springerplus* 5:18
45. Martin RM, Wright MJ, Lutkenhoff ES et al (2017) Traumatic hemorrhagic brain injury: impact of location and resorption on cognitive outcome. *J Neurosurg* 126:796–804